

A Receding Horizon Control for Linear System Subjected to Input Magnitude and Rate Saturation

Feng Tyan

Department of Aerospace Engineering
Tamshui, Taipei County, Taiwan 25147, R. O. C.
Phone: 886-2-2621-5656 ext. 2781
Email: 100740@mail.tku.edu.tw

Abstract

This paper proposes a static (LQR) plus a dynamic compensation scheme for input magnitude and rate constrained linear system to cope with the windup phenomenon. Given a linear static controller for such a linear system designed without considering its input constraints, an additional receding horizon type dynamic compensator based on Pontryagin's minimum principle is added to account for the constraints. To determine the required initial condition of the proposed dynamic compensator, a simple iterative scheme is also given in the context. Then the stability property of the resulting closed-loop system is investigated through a corresponding Lyapunov function.

Key Words

Receding horizon control, Pontryagin's minimum principle, magnitude saturation, rate saturation.

⁰This research was supported in part by the National Science Council, Taiwan, under grant NC-90-2213-E-032-010-.

1 Introduction

The input saturation problem is intrinsic to automatic control technology. In fact, no technological advance can circumvent rate and magnitude constraints on electromechanical actuator. Furthermore, cost constraints often force control engineers to extract the best possible performance from components with limited capability, thus increasing the occurrence of saturation. The importance and pervasiveness of saturation is reflected by the extensive research devoted to the problem. Among them only few researchers studied the problem of magnitude and rate saturation, for example: [1] (based on LMI), [2] (for neutrally stable system via error governor), [3] (QFT approach). In constructing the controller, receding horizon control (or model predictive control) were implemented quite often when the system subjected to input or(and) state constraints. However, most of the literatures dealt with only the discrete time system [4-7]. Only very few discuss continuous time system directly, but no constraint is involved [8] (A unified continuous/discrete time approach), [9]. See also [10] for a historical review and the references therein.

This paper proposes a static (LQR) plus a dynamic compensation scheme for input magnitude and rate constrained linear system to cope with the windup phenomenon. Given a linear static controller for such a linear system designed without considering its input constraints, an additional dynamic compensator based on Pontryagin's minimum principle (with a quadratic like cost functional) is added to account for the constraints. To determine the required initial condition of the proposed dynamic compensator, a simple iterative scheme is also given in the context. Then the stability property of the resulting closed-loop system is investigated through a corresponding Lyapunov function. Finally, a numerical example is given to compare the performance of the proposed method with that of the LQR controller.

NOTATION:

\mathbf{R}^n	set of $n \times 1$ real vectors
$\mathbf{P}^{n \times n}, \mathbf{DP}^{n \times n}$	set of $n \times n$ positive-definite matrices, diagonal positive-definite matrices
$\mathbf{N}^{n \times n}, \mathbf{DN}^{n \times n}$	set of $n \times n$ nonnegative-definite, diagonal nonnegative-definite matrices
$M \geq 0$	symmetric matrix M is positive semidefinite
$M > 0, M < 0$	symmetric matrix M is positive definite, negative definite, respectively

2 Controller Synthesis for Systems with Input Magnitude Constraint

Consider the completely controllable system shown in Figure 1.

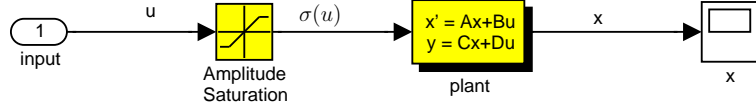


Figure 1: Linear System with Magnitude Saturation

The state space representation for this system can be written as

$$\begin{aligned} \dot{x}(t) &= Ax(t) + B\sigma(u(t)), \quad x(t_0) = x_0, \\ y(t) &= x(t), \end{aligned} \tag{2.1}$$

and the cost functional

$$J = \frac{1}{2} x^T(t_0 + T) Q_f x(t_0 + T) + \frac{1}{2} \int_{t_0}^{t_0 + T} \left[x^T Q x + u^T R_2 \sigma(u) \right] dt, \tag{2.2}$$

where $x \in \mathbf{R}^n, u \in \mathbf{R}^m$ and A, B are real matrices of compatible dimension, (A, B) is controllable, $Q_f \in \mathbf{N}^{n \times n}, Q \in \mathbf{N}^{n \times n}, R_2 \in \mathbf{DP}^{m \times m}$, and the finite horizon $T > 0$ is fixed. The function $\sigma : \mathbf{R}^m \rightarrow \mathbf{R}^m$ is an independent saturation function, that is,

$$\sigma(u) \triangleq [\sigma_1(u_1) \cdots \sigma_m(u_m)]^T, \tag{2.3}$$

where

$$\sigma_i(u_i) \triangleq \text{sat}(u_i), \quad i = 1, \dots, m, \tag{2.4}$$

and

$$\text{sat}(u_i) = \begin{cases} u_i, & \underline{u}_i \leq u_i \leq \bar{u}_i, \\ \bar{u}_i, & u_i > \bar{u}_i, \\ \underline{u}_i, & u_i < \underline{u}_i, \end{cases} \quad (2.5)$$

in which $\underline{u}_i < 0 < \bar{u}_i$ are the lower and upper bound of saturation function respectively. For $m \geq 2$ the saturation function $\sigma(\cdot)$ may change the direction of the control input, that is, $\sigma(u(t))$ is not necessarily in the same direction as $u(t)$.

For the convenience of analysis, the saturation function is written in the following form

$$\sigma(u) = (I - |S(u)|)u + |S(u)|u_s, \quad (2.6)$$

where

$$\begin{aligned} |S(u)| &\triangleq \text{diag}(|S_{11}(u_1)| \cdots |S_{mm}(u_m)|), \\ S_{ii}(u_i) &\triangleq \text{sgn}(u_i - \sigma_i(u_i)), i = 1, \dots, m, \\ \text{sgn}(u_i - \sigma_i(u_i)) &\triangleq \begin{cases} 1, & u_i > \sigma_i(u_i), \\ 0, & u_i = \sigma_i(u_i), \\ -1, & u_i < \sigma_i(u_i), \end{cases} \end{aligned} \quad (2.7)$$

and

$$\begin{aligned} u_s &\triangleq [u_{s_1} \cdots u_{s_m}]^T, \\ u_{s_i} &\triangleq \begin{cases} \bar{u}_i, & \text{if } S_{ii}(u_i) = 1, \\ \underline{u}_i, & \text{if } S_{ii}(u_i) = -1, \end{cases} \quad i = 1, \dots, m. \end{aligned} \quad (2.8)$$

In addition, it is easy to see that

$$\frac{\partial \sigma(u)}{\partial u} = I - |S(u)|, \quad (2.9)$$

for all u except that when $u = u_s$. Therefore, an alternative form of the system can be expressed as

$$\dot{x} = Ax + Bu - B|S(u)|(u - u_s). \quad (2.10)$$

To determine the optimal controller u , let us consider the corresponding Hamiltonian function

$$H(x, u, \lambda) = \frac{1}{2} [x^T Qx + u^T R_2 \sigma(u)] + \lambda^T [Ax + B\sigma(u)], \quad (2.11)$$

where λ is the corresponding costate. Next, let u represent the optimal controller, x and λ be the corresponding optimal state and costate, and v be any admissible control. Then apply the Pontryagin's minimum principle [11], we have

$$\begin{aligned}
H(x, u, \lambda) &\leq H(x, v, \lambda), \\
&\Leftrightarrow \frac{1}{2}u^T R\sigma(u) + \lambda^T B\sigma(u) \leq \frac{1}{2}v^T R_2\sigma(v) + \lambda^T B\sigma(v), \\
&\Leftrightarrow \frac{1}{2}[\sigma(u) + R_2^{-1}B^T\lambda]^T R_2[\sigma(u) + R_2^{-1}B^T\lambda] + \frac{1}{2}\sigma^T(u)R_2[u - \sigma(u)] \\
&\leq \frac{1}{2}[\sigma(v) + R_2^{-1}B^T\lambda]^T R_2[\sigma(v) + R_2^{-1}B^T\lambda] + \frac{1}{2}\sigma^T(v)R_2[v - \sigma(v)], \\
&\Leftrightarrow \frac{1}{2}[u + R_2^{-1}B^T\lambda]^T R_2[u + R_2^{-1}B^T\lambda] - [u - \sigma(u)]^T R_2[u + R_2^{-1}B^T\lambda] \\
&\leq \frac{1}{2}[v + R_2^{-1}B^T\lambda]^T R_2[v + R_2^{-1}B^T\lambda] - [v - \sigma(v)]^T R_2[v + R_2^{-1}B^T\lambda],
\end{aligned} \tag{2.12}$$

which in turn shows that the optimal controller u that satisfies the magnitude constraint (2.5) takes the same form as in the unconstrained case

$$u = -R_2^{-1}B^T\lambda, \tag{2.13}$$

where the costate λ satisfies the differential equation

$$\dot{\lambda} = -\frac{\partial H}{\partial x} = -Qx - A^T\lambda, \quad \lambda(t_0 + T) = Q_f x(t_0 + T). \tag{2.14}$$

In order to attempt to determine a closed-loop control, we assume

$$\lambda = Px + \xi. \tag{2.15}$$

Substitute this relation into equation (2.14) and determine the requirements for a solution. After some manipulations, we easily obtain the following requirement:

$$0 = (\dot{P} + PA - PBR_2^{-1}B^T P + A^T P + Q)x + \dot{\xi} + (A - BR_2^{-1}B^T P)^T \xi - PB|S(u)|(u - u_s). \tag{2.16}$$

Because this must be satisfied for all $x(t)$ and $u(t)$, we conclude that

$$\dot{P} = -PA - A^T P + PBR_2^{-1}B^T P - Q, \quad P(t_0 + T) = Q_f, \tag{2.17}$$

$$\dot{\xi} = -(A + BK_x)^T \xi - K_x^T R_2 |S(u)|(u - u_s), \quad \xi(t_0 + T) = 0, \tag{2.18}$$

where

$$K_x \triangleq -R_2^{-1}B^T P. \quad (2.19)$$

For simplicity, we choose $Q_f = P_\infty$, where P_∞ satisfies the algebraic Riccati equation

$$0 = P_\infty A + A^T P_\infty - P_\infty B R_2^{-1} B^T P_\infty + Q. \quad (2.20)$$

Apparently, in this case the solution to differential equation (2.17) is $P(t) = P_\infty, t_0 \leq t \leq t_0 + T$. The only remaining unknown is the initial condition $\xi(t_0)$. To this end, we propose the following simple iterative scheme in each finite horizon $t_0 \leq t \leq t_0 + T$:

Numerical Algorithm:

Step 0 Set counter $i = 0$, choose initial guess $\xi(t_0)_i = 0$, select tolerance ε , finite horizon T .

Step 1 Integrate (2.1), (2.18) with controller

$$u = K_x x + K_\xi \xi, \quad (2.21)$$

where

$$K_\xi \triangleq -R_2^{-1}B^T. \quad (2.22)$$

Step 2 Store the predicted control history $u(t), \sigma(u(t))$ for $t_0 \leq t \leq t_0 + T$,

Step 3 Implement the stored control history in Step 2, integrate (2.18) backwardly to obtain the updated $\xi(t_0)_{i+1}$.

Step 4 If $\|\xi(t_0)_i - \xi(t_0)_{i+1}\| < \varepsilon$ then stop, otherwise set $i = i + 1$, go to Step 1.

The closed-loop system configuration is shown in Figure 2. Note that the initial condition of ξ is updated in every predetermined time interval.

3 Controller Synthesis for Systems with Magnitude and Rate Saturation Nonlinearities

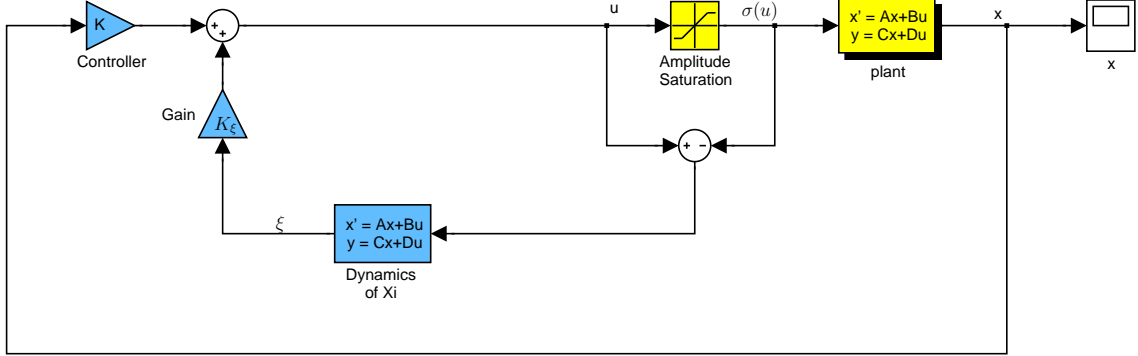


Figure 2: Closed System Configuration of System with Model Predictive Controller.

Consider the n th-order plant shown in Figure 3 subjected to both magnitude and rate saturation $\sigma_{rs}(\cdot)$ given by

$$\begin{aligned} \dot{x}(t) &= Ax(t) + B\sigma_{rs}(u(t)), \\ y(t) &= x(t). \end{aligned} \quad (3.1)$$

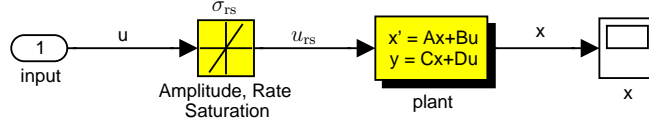


Figure 3: Linear System with Magnitude and Rate Saturation

The magnitude-rate saturation function $\sigma_{rs}(\cdot)$ in (3.1) is given in more detail in Figure 4 [12].

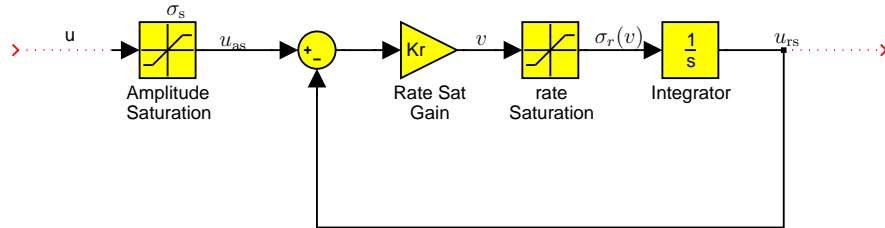


Figure 4: Magnitude, Rate Saturation Model $\sigma_{rs}(u)$

The magnitude saturation σ_s shown in Figure 4 is defined as in Section 2. For convenience, we use the shorthand notation $u_{as}(t)$ to denote $\sigma_s(u(t))$ and $u_{rs}(t)$ to denote $\sigma_{rs}(u(t))$ respectively. In addition, $u_{as} \in \mathbf{R}^m$, $v \in \mathbf{R}^m$, $u_{rs} \in \mathbf{R}^m$, $K_r = \text{diag}(K_{r1}, \dots, K_{rm})$, $K_{ri} \gg 1$, $i = 1, \dots, m$,

$$\sigma_r(v) \triangleq [\sigma_{r1}(v_1) \cdots \sigma_{rm}(v_m)]^T, \quad (3.2)$$

and

$$\sigma_{ri}(v_i) \triangleq \text{sat}(v_i), \quad i = 1, \dots, m, \quad (3.3)$$

where $\underline{v}_i \leq \text{sat}(v_i) \leq \bar{v}_i$, the rate saturation levels. $\underline{v}_i < 0, 0 < \bar{v}_i, i = 1, \dots, m$, The rate saturation model shown in Figure 4 is a closed-loop position-feedback-type model with dynamics

$$\dot{u}_{rs}(t) = \sigma_r(K_r[u_{as}(t) - u_{rs}(t)]), \quad u_{rs}(0) = u_{rs0}. \quad (3.4)$$

As the gain K_r increases, the output from the rate saturation model (3.4) converges to the output of the rate limiter model of Simulink [12].

The aim of this section is to determine an optimal controller $u(t)$ such that the performance index (3.5) can be minimized.

$$J = \frac{1}{2}x^T(t_0 + T)P_\infty x(t_0 + T) + \frac{1}{2} \int_{t_0}^{t_0+T} \left[x^T Q x + u^T R_2 \sigma_{rs}(u) \right] dt, \quad (3.5)$$

where P_∞ satisfies equation (2.20), $Q \in \mathbf{N}^{n \times n}$, $R_2 \in \mathbf{DP}^{m \times m}$, and the finite horizon $T > 0$ is fixed. As shown in [12], the magnitude of the magnitude-rate saturation model (3.4) is also bounded by the saturation level of $\sigma_s(\cdot)$. Hence, if we follow the similar procedure as given in Section 2, the optimal controller can be obtained in the same form again

$$u = K_x x + K_\xi \xi, \quad (3.6)$$

where K_x and K_ξ are defined by equations (2.19) and (2.22) respectively, and ξ satisfies

$$\dot{\xi} = -(A + BK_x)^T \xi - K_x^T R_2 [u - \sigma_{rs}(u)], \quad \xi(t_0 + T) = 0. \quad (3.7)$$

The corresponding closed-loop configuration is shown in Figure 5

4 Stability Analysis of the Receding Horizon Control

To save space, we consider the stability analysis of linear system subjected to only input magnitude constraint. For the case of both input magnitude and rate constraint follows a similar argument shown in this section. Let the optimal cost functional at $x(t)$ be

$$V(x(t)) \triangleq \frac{1}{2}x^T(t_0 + T)Q_f x(t_0 + T) + \frac{1}{2} \int_t^{t_0+T} \left[x^T Q x + u^T R_2 \sigma(u) \right] dt. \quad (4.1)$$

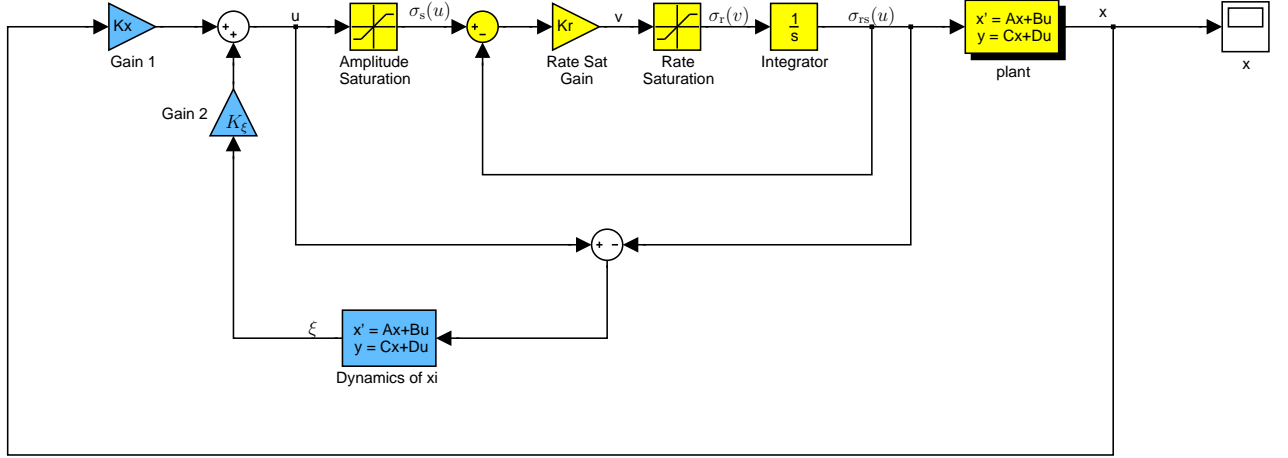


Figure 5: Closed System Configuration of Linear System with Magnitude and Rate Saturation.

For the state initial condition $x(t)$, if there exists the initial condition $\xi(t)$ such that $\xi(t+T) = 0$, we claim that the optimal cost functional at $x(t)$ is indeed a Lyapunov function and can be expressed as the product of state x and costate λ

$$V(x) = \frac{1}{2} x^T \lambda = \frac{1}{2} x^T (P_\infty x + \xi). \quad (4.2)$$

This can easily be verified by using the fact that both equations (4.1) and (4.2) render the same differential equation

$$\dot{V}(x) = -\frac{1}{2} \left[x^T Q x + u^T R_2 \sigma(u) \right] \leq 0, \quad (4.3)$$

with the same terminal condition

$$V(x(t_0 + T)) = \frac{1}{2} x^T(t_0 + T) Q_f x(t_0 + T). \quad (4.4)$$

In addition, it is can be shown that

- $V(x)$ is positive definite, that is $V(x) > 0, \forall x \neq 0$, and $V(x) = 0$ only for $x = 0$.
- The set $\{x : \dot{V}(x) = 0\}$ contains only $x = 0$.

This shows that the proposed optimal controller stabilize the system (2.1) asymptotically.

5 Numerical Example

Example 5.1. Consider an unstable system containing double poles at $j\omega$ axis,

$$\dot{x}(t) = \begin{bmatrix} 0 & 1 & 0 & 0 \\ 0 & 0 & 1 & 0 \\ 0 & 0 & 0 & 1 \\ -1 & 0 & -2 & 0 \end{bmatrix} x(t) + \begin{bmatrix} 0 \\ 0 \\ 0 \\ 1 \end{bmatrix} \sigma(u(t)), \quad x(0) = \begin{bmatrix} -2 \\ -20 \\ -4 \\ 1 \end{bmatrix}.$$

The control action is bounded as follows: $\bar{u} = -\underline{u} = 5$, $\bar{v} = -\underline{v} = 20$, respectively. The controller is required to drive the system state to the origin from the initial state $x(0)$. Tuning

parameters for the controller are the state weighting $Q = \begin{bmatrix} 1 & 0 & 0 & 0 \\ 0 & 1 & 0 & 0 \\ 0 & 0 & 1 & 0 \\ 0 & 0 & 0 & 1 \end{bmatrix}$, and controller

weighting $R_2 = 1$, receding horizon $T = 5$. For every 0.01 second, the receding horizon controller is implemented. Figures 6,7 show the system response of the closed system using LQR and RHC respectively. In both of thses two figures only the magnitude constraints are considered (the saturation levels are $\bar{u} = -\underline{u} = 5$). Then we add rate saturation in both of the systems shown in Figures 8 and 9 (the rate saturation levels are $\bar{v} = -\underline{v} = 20$). From the above comparison, it is easy to see the superioty of the proposed controller (at the cost of some CPU time).

6 Conclusion

In this paper, for a static (LQR) type controller designed for unconstrained linear system, we presented a receding horizon type dynamic compensator based on Pontryagin's minimum principle to cope with the windup phenomenon. To determine the optimal controller, a quadratic type performance index is used. As in most optimal control problem, the initial condition of the costate is a key issue. To determine the required initial condition of the proposed dynamic compensator, a simple iterative scheme is also given in the context. Then the stability

property of the resulting closed-loop system is investigated through a corresponding Lyapunov function. Finally, in the numerical example, we see that the added dynamic controller provides the information to account for the windup phenomenon.

Acknowledgements

This work is supported in part by the National Science Council, Taiwan, under the Grant NSC 90-2213-E-032-010.

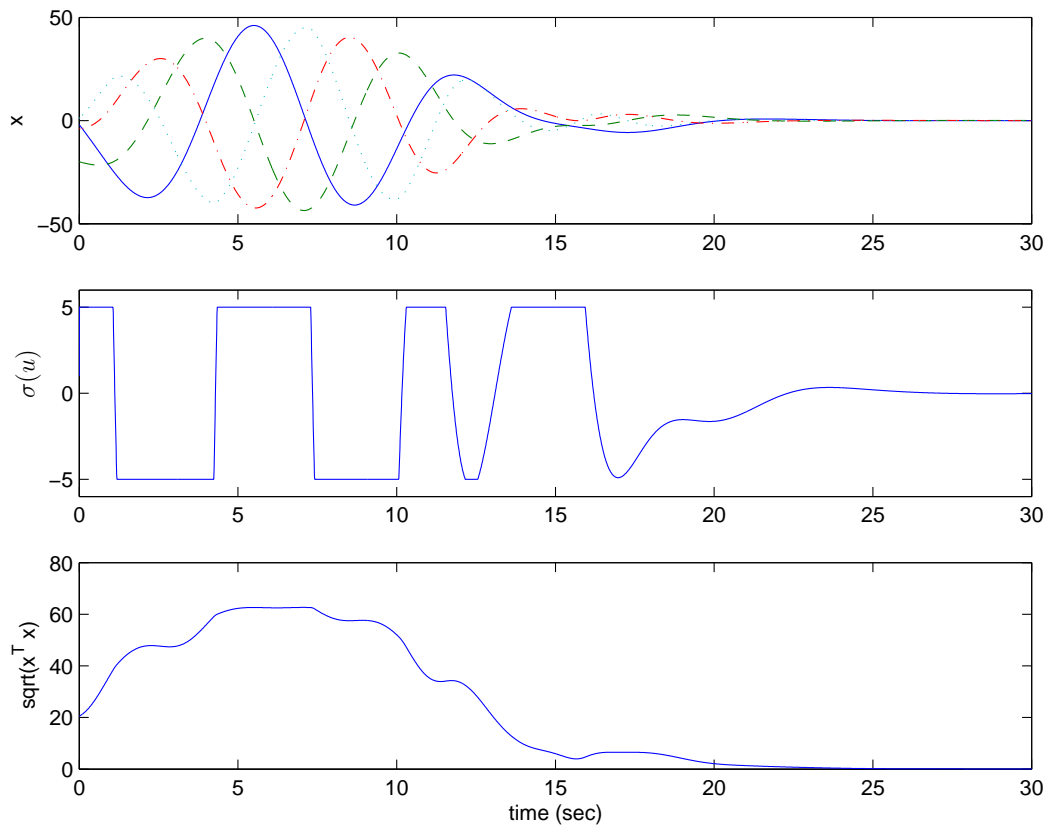


Figure 6: Response of the system given in Example 5.1 with LRQ Controller, $\bar{u} = -\underline{u} = 5$.

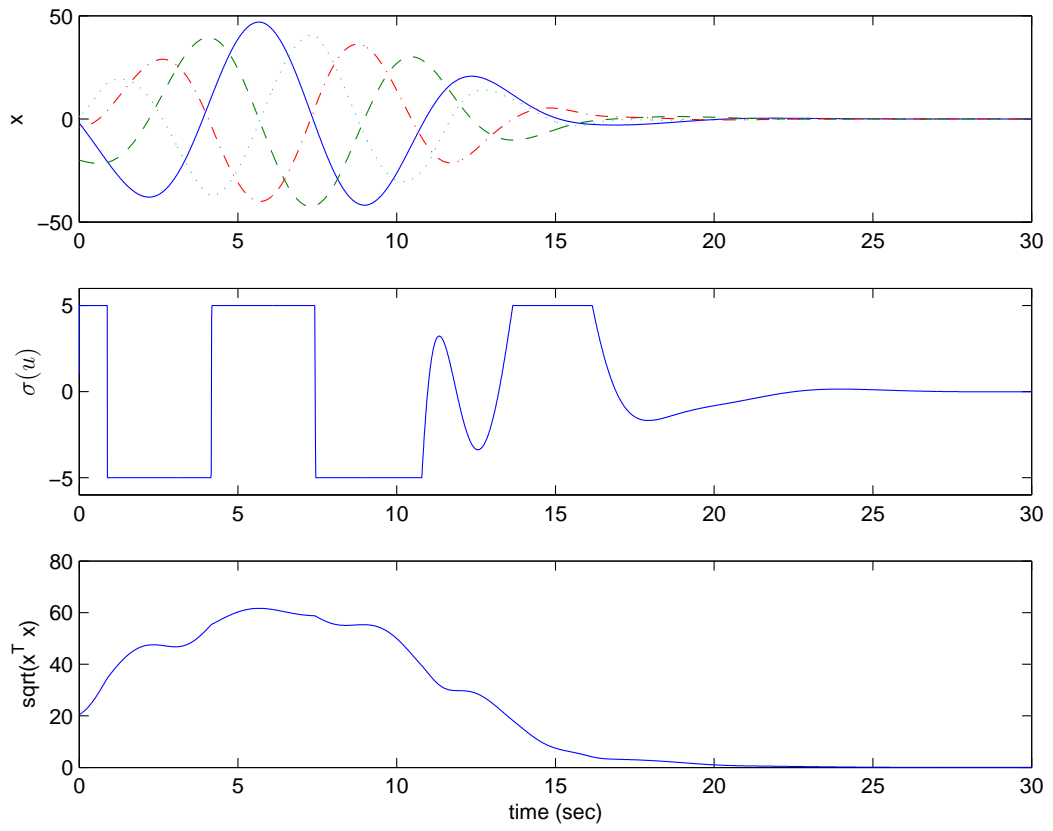


Figure 7: Response of the system given in Example 5.1 with RH Controller, $T = 5$, $\bar{u} = -\underline{u} = 5$.

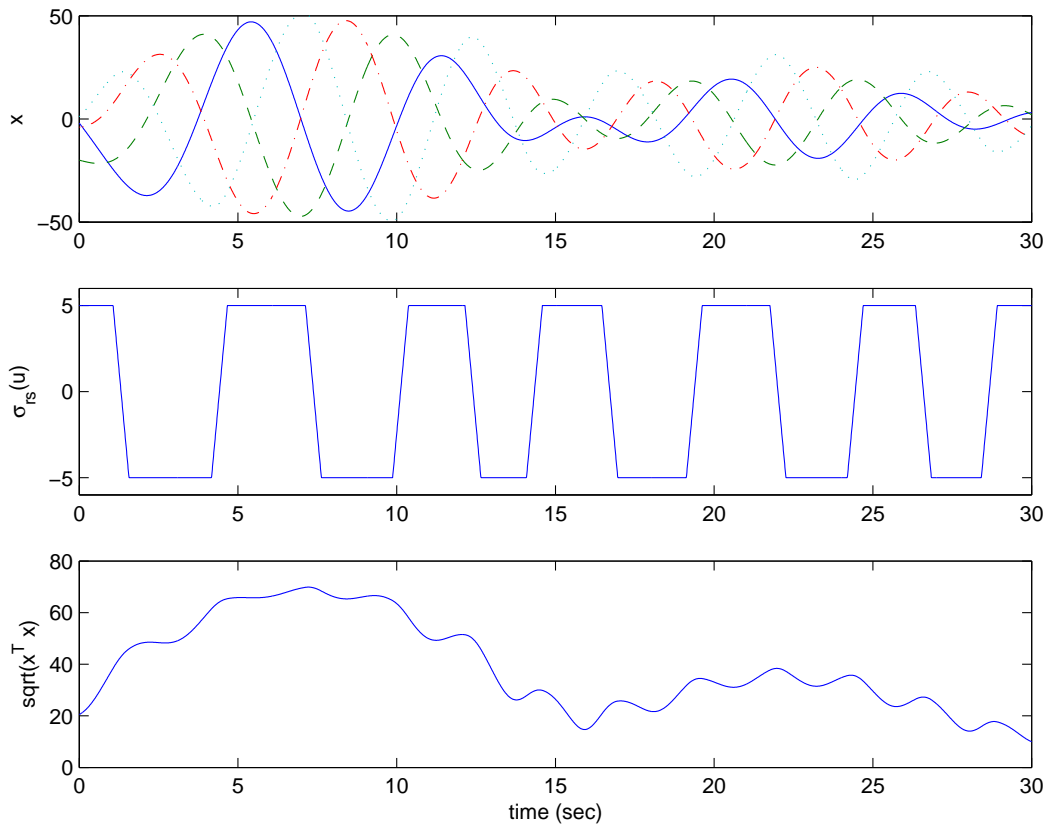


Figure 8: Response of the system given in Example 5.1 with LQR Controller, $\bar{u} = -\underline{u} = 5$, $\bar{v} = -\underline{v} = 20$.

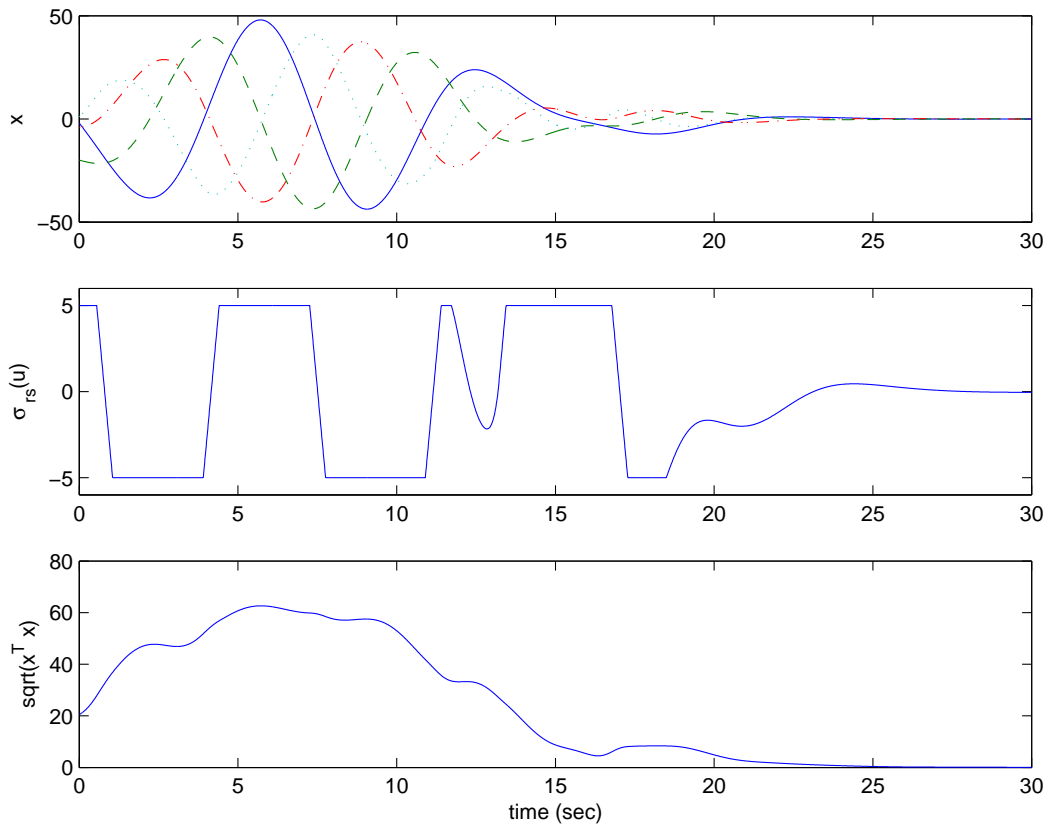


Figure 9: Response of the system given in Example 5.1 with RH Controller, $T = 5$, $\bar{u} = -\underline{u} = 5$, $\bar{v} = -\underline{v} = 20$.

References

- [1] İ. Emre Köse and F. Jabbari, “Rate and Magnitude-Bounded Actuators: Scheduled State Feedback Design,” in *15th Triennial World Congress*, (Barcelona, Spain), 2002 IFAC, 2002.
- [2] P. Kamasouris and M. Athans, “Control Systems with Rate and Magnitude Saturation for Neurally Stable Open Loop System,” in *Proceedings of the 29th Conference on Decision & Control*, (Honolulu, Hawaii, U. S. A.), pp. 3404–3409, 1990 CDC, December 1990.
- [3] W. Wu and S. Jayasuriya, “A QFT Design Methodology for Feedback Systems with Input Rate or Amplitude Rate Saturation,” in *Proceedings of the American Control Conference*, (Arlington, VA, U. S.A.), pp. 378–385, 2001 ACC, June 25-27 2001.
- [4] A. Bemporad, F. Borrelli, and M. Morari, “The Explicit Solution of Constrained LP-Based Receding Horizon Control,” in *Proceedings of the 39th Conference on Decision & Control*, (Sydney, Australia), pp. 632–637, 2000 CDC, December 2000.
- [5] T. A. Johansen, I. Petersen, and O. Slupphaug, “On Explicit Suboptimal LQR with State and Input Constraints,” in *Proceedings of the 39th Conference on Decision & Control*, (Sydney, Australia), pp. 662–667, 2000 CDC, December 2000.
- [6] W. B. Dunbar, M. B. Milam, R. Franz, and R. M. Murray, “Model Predictive Control of a Thrust-Vectored Flight Control Experiment,” in *15th Triennial World Congress*, (Barcelona, Spain), 2002 IFAC, 2002.
- [7] D. E. Quevedo, J. A. D. Doná, and G. C. Goodwin, “Receding Horizon Linear Quadratic Control with Finite Input Constraint Sets,” in *15th Triennial World Congress*, (Barcelona, Spain), 2002 IFAC, 2002.
- [8] M. Bouslimani, M. M’Saad, and L. Dugard, “Stabilizing Receding Horizon Control: A Unified Continuous/ Discrete Time Formulation,” in *Proceedings of the 32nd Conference on Decision & Control*, (San Antonio, Texas, U. S. A.), pp. 1298–1303, 1993 CDC, December 1993.

- [9] K. B. Kim, T.-W. Yoon, and W. H. Kwon, "Receding Horizon Guidance Laws for Constrained Missiles with Autopilot Lags," *Control Engineering Practice*, vol. 9, pp. 1107–1115, 2001.
- [10] D. S. Bernstein and A. N. Michel, "A Chronological Bibliography on Saturating Actuators," *International Journal of Robust and Nonlinear Control*, vol. 5, pp. 375–380, 1995.
- [11] M. Athans and P. L. Falb, *Optimal Control: An Introduction to the Theory and Its Applications*. New York: McGraw-Hill, 1966.
- [12] F. Tyan and D. S. Bernstein, "Dynamic Output Feedback Compensation for Systems with Independent Amplitude and Rate Saturation," *International Journal of Control*, vol. 47, no. 1, pp. 89–116, 1997.

7 Appendix: MATLAB Codes

```
%
% system_data file for Receding Horizon Control
%
clear all;

% plant parameters

Ap=[0 1 0 0;
    0 0 1 0;
    0 0 0 1;
    -1 0 -2 0];
Bp=[0 0 0 1]';
%Bp=[0 0 0 1]';
[xdim,mAp]=size(Ap);
[nBp,udim]=size(Bp);
Cp=eye(xdim,xdim);
Dp=zeros(xdim,udim);
xp0=[-2 -20 -4 1]';
xp=xp0;
yp(:,1)=Cp*xp;

Q=eye(xdim,xdim);
R=eye(udim,udim);
S=zeros(xdim,udim);
[K,P]=lqr(Ap,Bp,Q,R,S);
K=-K;

% K=[-1 -1 -2 -1];
```

```

% x1(0)=-2,x2(0)=-1,x3(0)=-4,x4(0)=1;
% x1(0)=-2,x2(0)=-20,x3(0)=-4,x4(0)=1;

N=R;

Axi=-(Ap+Bp*K)';
Bxi=P*Bp;
Cxi=eye(xdim,xdim);
Dxi=zeros(xdim,udim);
xif=zeros(xdim,1); % final value of xi
xi0=xif; % initial guess of xi
xi=xi0; % innitial guess of xi
Kxi=-inv(R)*Bp';

%
% magnitude saturation level
%
umax=5*ones(udim,1);
umin=-umax;
%
% rate saturation level
%
vmax=20*ones(udim,1);
vmin=-vmax;

input2xp(:,1)=sat(K*xp,umin,umax);
ypnorm(1)=norm(yp(:,1));
%
% auxiliary system parameters
%
```

```

t0=0; i=1; % initial time
tf=30; % final time
trecede=5; % recede horizon time span
h=1e-2; % max. time step
hmin=h/10; % min. time step
tol=1e-7; % tolerance in numerical integrator
options = odeset('RelTol',1e-4,'AbsTol',tol,'MaxStep',h);
rtime=linspace(t0,tf,round((tf-t0)/trecede)+1); % total time span for RH
time=linspace(t0,tf,round((tf-t0)/h)+1); % total time span
itime=length(time);

%
% construct state space model
sysxp=ss(Ap,Bp,Cp,Dp);
sysxi=ss(Axi,Bxi,Cxi,Dxi);
sysxib=ss(-Axi,-Bxi,Cxi,Dxi);

% convert to discrete sytem
[sysxpd,Gp]=c2d(sysxp,h,'zoh');
[sysxid,Gxi]=c2d(sysxi,trecede/20,'zoh');
[Apd, Bpd] = ssdata(sysxpd); % discrete system
[Axid, Bxid] = ssdata(sysxid); % discrete system

```

```

%
% MAIN PROGRAM
%

clear all;

%
% load system data
%

system_data_5;
trecede=2;

simopt5ps=simset('Solver','ode5','FixedStep',hmin);
simopt5rs=simset('Solver','ode45','MaxStep',hmin);

for it=1:itime-1
tspan=[time(it) time(it+1)];
%
% receding horizon
%

    for iiter=1:20
        xiold=xi;
        % predict u and sat(u)
        [recedespan,dummy,u,satu]=sim('forward_5ps',[0 trecede],simopt5ps);
        revinput=[reverse(trecede-recedespan,'r') reverse((u-satu),'r')];
        %
        % estimated I.C. of xi
        xiout=lsim(sysxib,reverse((u-satu)'),'c'),recedespan,xif); xiout=xiout';
        % [dummy,dummy,xiout]=sim('backward_5s',[0 trecede],simopt5rs,revinput); xiout=xiout';

```

```

xi=xiout(:,end);

xierror=norm(xi-xiold);

xiff=lsim(sysxi,(u-satu),recedespan,xi); xiff=xiff'; xif0=xiff(:,end);
if (xierror < 1e-7);
%   if (norm(xif0) < 1e-9);
    break;
end;
end;

[tdummy,dummy,y1,y2,y3,y4]=sim('forward_5rs',tspan,simopt5rs);
y1=y1'; y2=y2'; y3=y3'; y4=y4';
input2xp(:,it+1)=y1(:,end); % input history
dt=time(it+1)-time(it); previousinput=input2xp(:,it);
yp(:,it+1)=y2(:,end);
ypnorm(it+1)=y3(end);
xp=yp(:,it+1); xi=y4(:,end);

    [time(it+1)  norm(xif0)  ypnorm(it+1) (input2xp(:,it+1)-previousinput)/dt]
end;

figure(1);
subplot(311); plot(time,yp'); ylabel('x')
subplot(312); plot(time,input2xp');
subplot(313); plot(time,ypnorm); ylabel('sqrt(x^T x)')
xlabel('time (sec)')
shg;

```

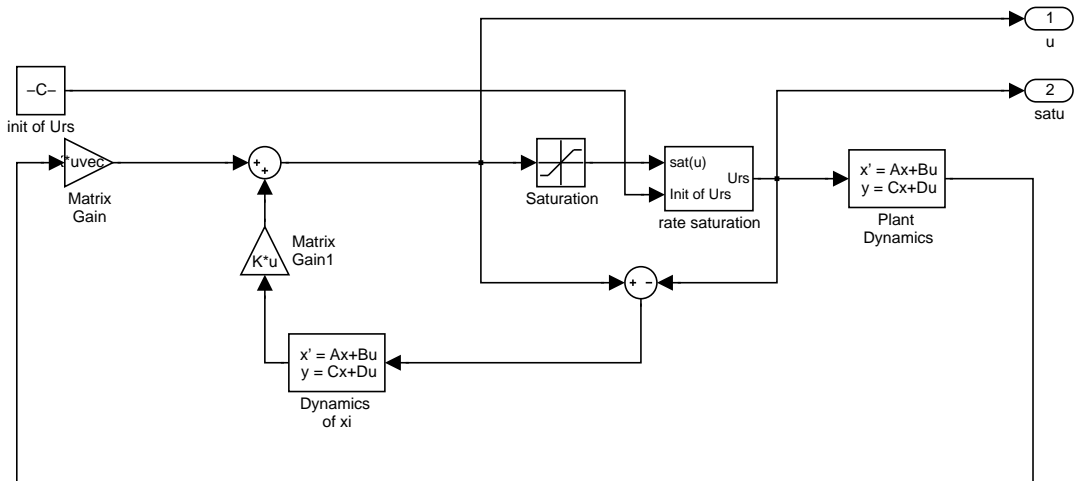


Figure 10: The SIMULINK diagram of forward-5ps.mdl

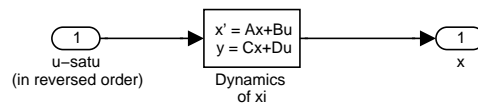


Figure 11: The SIMULINK diagram of backward-5s.mdl

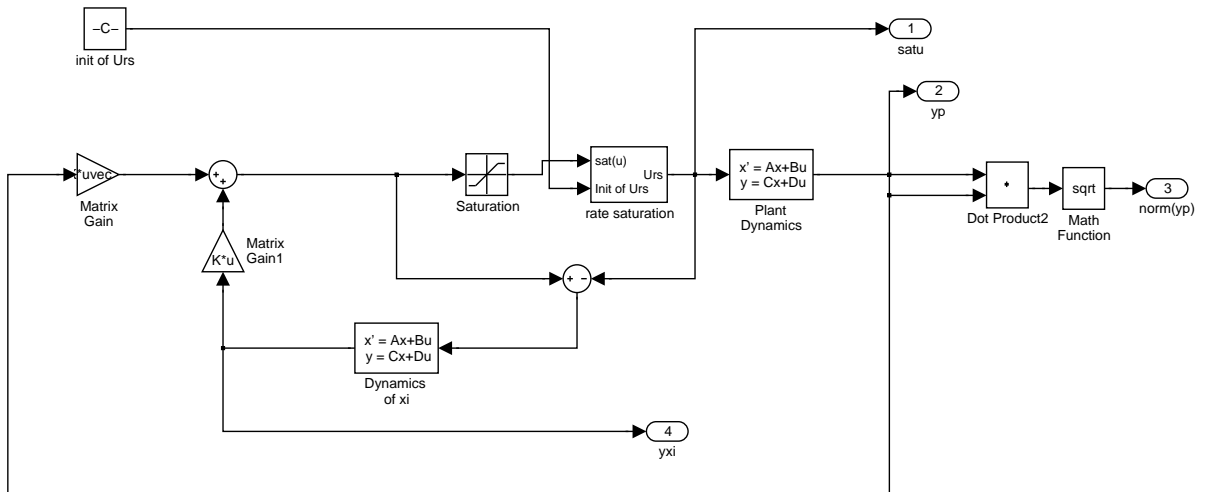


Figure 12: The SIMULINK diagram of forward-5rs.mdl